Journal of Engineering Research

Volume 7 | Issue 2 Article 3

2023

Design and Implementation of an ADCS for a CubeSat

Sara Fouad Mohamed

Follow this and additional works at: https://digitalcommons.aaru.edu.jo/erjeng

Recommended Citation
Fouad Mohamed, Sara (2023) "Design and Implementation of an ADCS for a CubeSat," *Journal of Engineering Research*: Vol. 7: Iss. 2, Article 3.
Available at: https://digitalcommons.aaru.edu.jo/erjeng/vol7/iss2/3

This Article is brought to you for free and open access by Arab Journals Platform. It has been accepted for inclusion in Journal of Engineering Research by an authorized editor. The journal is hosted on Digital Commons, an Elsevier platform. For more information, please contact rakan@aaru.edu.jo, marah@aaru.edu.jo, u.murad@aaru.edu.jo.

Erjeng: Engineering Research (ERJENG)
Vol. 7 – No. 2, 2023
©Tanta University, Faculty of Engineering
ISSN: 2356-9441 https://erjeng.journals.ekb.eg/ e ISSN: 2735-4873

Design and Implementation of an ADCS for a CubeSat

Sara Fouad[1*†], M. Abd Elghany[2], Lamia Mostafa[2] ,M. Abd El salam[2], Abd Elmonuim El Mahdy[1], and Ahmed H. Eldeeb[3*†](Senior Member in IEEE)

[1*]Electronic and Communication Department, Modern Academy for Engineering & Technology, Mokatam, Cairo, Egypt. – sarafouad2012.s.m.a@gmail.com.
[2] Electronic and Communication department, Egyptian Space Agency, New Capital, Cairo, Egypt.
[3*] Electronic and Communication Department, Gezira Higher Institute of Engineering and Technology (EGI). Cairo, Egypt– ahmed.eldeib@gmail.com.

***Abstract*- The hardware implementation of the attitude determination process of the Attitude Determination Control Subsystem (ADCS) for CubeSat is presented in this paper. The process of determining attitude involves combining data from several sensors that monitor internal or external references. ADCS has four primary subsystems; the sensor system, the actuator system, the controller, and the interface. The proposed ADCS is based on implementing the controller and sensor subsystems to monitor attitude determination. The STM32F405 microcontroller is used on the board as the main controller. External circuits are designed on the board to be compatible with the microcontroller and ADCS functions. The supplied circuit feeds the board from the voltage supplied by six panels of solar cells. The step-down feeding board circuit and the step-down STM feeding circuit are designed to create a suitable step-down supply voltage. Two oscillators are designed, which are needed in the STM32F405 microcontroller. The three intended H-bridge drives are implemented for use with brush motors. A joint action group (J-Tag) is connected to debug the device. The ADCS board's sensors subsystem included a magnetometer, temperature, and gyroscope sensors. The ADCS board circuits are simulated using Altium and fabricated On-Board Circuit (OBC) in small dimensions of 10×9.7 cm^2.**

***Keywords*- Attitude determination, CubeSat, Attitude determination control subsystem, onboard circuit**

I. INTRODUCTION

The development of small satellites has improved significantly aerospace engineering. This increase has been made possible by the notable decrease in cost and development time, which may be explained by a number of causes, one of which is the huge advancements in microelectronics and integrated technologies. Small satellites like CubeSats have progressed from being seen as toys and mainly used for teaching to being reliable platforms for carrying out space missions. They have been employed for commercial [1, 2], government and military [3, 4], legitimate scientific [5, 6], and educational [7, 8] objectives. Currently, small satellite constellations are being launched for imaging and other data collection applications.

These CubeSats are classified as a class of Nanosatellites with sizes starting at $10\times10\times10$ cm^3 and going up in 10-cm length increments [9-12]. The satellite's on-orbit functioning includes a crucial subsystem for Attitude Determination Control Subsystem (ADCS). It has a significant impact on how well satellites perform. It can be exceedingly challenging to test an attitude determination and control subsystem ADCS since it may be necessary to use attitude dynamics and the orbital space environment.

The ADCS, as its names imply, is the system that determines and manages the CubeSat's position and orientation in orbit [13]. It can be split into four major subsystems: the interface, the controller, the actuator, as well as the sensor. The system that unites sensors and actuators is known as a controller. In order to achieve the intended orientation, it calculates the positioning from the data acquired, compares it to the desired position, and determines the rotations to apply to the actuators [14]. The ADCS hardware consists of the interface. Its primary function is the transmission of information from the sensors to the microcontroller and from the microcontrollers to the actuators. The sensor system consists of all the elements that collect data necessary for the ADCS to operate. This comprises sensors that monitor temperature as well as orientation and placement as well as velocity. The basic satellite sensors are a gyroscope, gyro meter, star trackers, sun sensors, magnetometers, and temperature sensors. All the elements that move the CubeSat are included in the actuator system. They involve rotations about the three axes of roll, pitch, and yaw. The basic satellite actuators are magnetorquers, reaction wheels, and a control momentum gyroscope [14].

The most related works were to demonstrate how hardware and software attitude knowledge and control develop over time in small satellites. The Institute for Space Studies at the University of Toronto's CanX2 satellite, which was developed in 2008, was one of the first to try attitude control. To determine its attitude, it uses a magnetometer, sun sensors, and magnetorquers. One reaction wheel developed by Sinclair is also used, which revolves around the device's long axis [15]. The pair of CubeSats with active attitude control was funded by the Naval Research Laboratory and was known as Qb-X1 and Qb-X2.

In this research [16], real-time attitude control using modified proportional-integral (MPI) attitude control on a hardware-in-the-loop (HIL) platform is presented for the microsatellite (MS) attitude determination and control system (ADCS). With the help of this platform, researchers can create novel, quick, and reliable controllers for space tests without incurring the significant expenses associated with employing genuine hardware for satellite attitude control.

MS needs precise ADCS and attitude drift regulation due to the rising need for small satellites in orbit. The measuring of MS's present attitude, the MS's attitude is estimated, and the MS's attitude is corrected accurately by using MPI's attitude controller. Without controller gain parameters, this controller has a straightforward design.

DOI: 10.21608/ERJENG.2023.197719.1160

Published by Arab Journals Platform, 2023

Journal of Engineering Research (ERJ)
Vol. 7 – No. 2, 2023
©Tanta University, Faculty of Engineering
https://erjeng.journals.ekb.eg/
ISSN: 2356-9441
e ISSN: 2735-4873

The accuracy of the ADCS simulated model is 0.01 degrees with regard to attitude inaccuracy. The study [17] presented a hardware implementation of an ADCS for two-axis-stabilized CubeSats that is adaptable and inexpensive. A novel Simplified Intelligent Proportional-Integral (SIPI) attitude control algorithm is included in the proposed ADCS to accurately modify the attitude. The attitude determination element of the system estimates CubeSat's present attitude. There is no controller gain parameter in the control algorithm, which is based on the multi-degree-of-freedom controller concept. The comparative attitude is read from the suggested ADCS based on a magnetometer, sun sensor, and Micro Electro Mechanical Sensor (MEMS) gyroscope, which is used to update the estimated attitude sent to the Kalman filter for calculating the attitude and angular velocity of the CubeSat. By using Matlab/Simulink and hardware implementation, the ADCS model is verified and validated.

This paper presents the hardware implementation of the attitude determination platform for ADCS. The main purpose of the ADCS board is to be designed on board to be compatible in dimension with CubeSat.

The main hardware components of the ADCS board are:

1. The STM32F405 is used as the microcontroller, which is the main brain of the board.
2. The feeding board circuit uses the regulator (XC6210B332MR) by taking the 5V output voltage from six panels of the solar cell; the regulator output will then be 3.3V.
3. A STM32 feeding circuit is created to step down the supplied voltage to the STM.
4. An amplifier called the LM P7704MT amplifies the voltage produced by the solar cells when they are connected to one another via a pico-blade.
5. The gyroscope, magnetometer, and temperature sensors are connected to the board.
6. The gyroscope sensor is used to measure 3-axis attitude determination.
7. The ADCS board circuits are simulated using Altium and fabricated On-Board Circuit (OBC) in small dimensions of 10×9.7 cm^2.

The structure of the paper, based on Section II, presents the hardware implementation of external circuits in ADCS; Section III describes the sensors that are used in the ADCS system, Section IV presents the hardware implementation of the ADCS OBC, and Section V depicts the microcontroller's software interface.

II. ADCS STRUCTURE

The ADCS is vital for CubeSat applications since it is the component that regulates the orientation of the CubeSat in space. Actuators, sensors, and a microprocessor with algorithms make up the ADCS [14]. The primary objective of the ADCS is to record the initial angular momentum and random rotation during the deployment, identify the CubeSat's attitude, and either maintain or change the CubeSat's attitude in accordance with the satellite's information. There are two primary functioning parts of the ADCS system. These two processes are Attitude Determination (AD), which utilizes sensor output to calculate the CubeSat's existing attitude, and attitude control, which determines the control signal produced by the actuator.

The proposed hardware components of the ADCS system are presented in this section as shown in figure 1. STM32F405 [18] is the main controller on board, it consists of 144 pins which are divided into groups of pins that have the same function to make it easy connection as shown in Figure 2. The main implemented elements used in the hardware board are a feeding board circuit using regulator "XC6210B332MR" by taking the 5V output voltage from the other board then regulator output will be 3.3V, As the STM32F405 contained a 15-pin power supply so STM feeding circuit is created to step down voltage. The STM32F405 is compatible with two oscillators. The first one of the oscillators works at 8MHz and 32 MHz as the second oscillator. An amplifier called the "LM P7704MT" amplifies the voltage produced by the solar cells when they are connected to one another via a pico-blade.

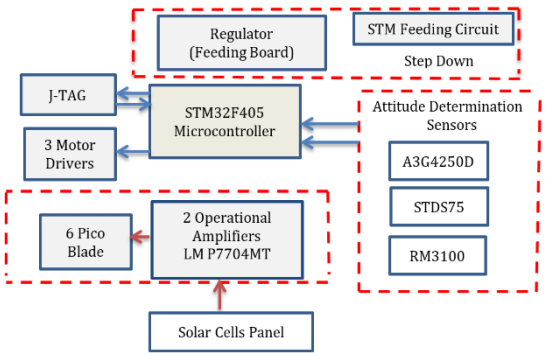

Figure 1. The basic structure of the proposed ADCS

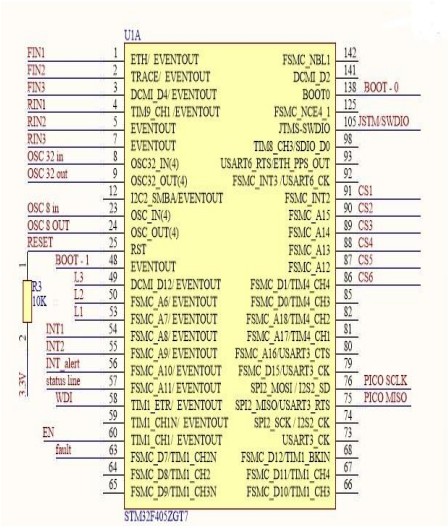

Figure 2. Connection pins of STM32F405 in Altium.

A joint action group (J-Tag) used as easily debug the device. The three H-bridge drivers are full-bridge drivers intended for use with brush motors. The gyroscope, magnetometer, and temperature sensors are connected to the board.

DOI: 10.21608/ERJENG.2023.197719.1160

Journal of Engineering Research (ERJ)
Vol. 7 – No. 2, 2023
©Tanta University, Faculty of Engineering
ISSN: 2356-9441 https://erjeng.journals.ekb.eg/ e ISSN: 2735-4873

The novelty of our work can be summarized in the following points:

1-The proposal is based on the design on board ADCS using the feature STM32F405 microcontroller.

2. The measurement of attitude determination is proposed using their axis gyroscope sensor.

3. The supplied circuit feeding the board is designed to be supplied by six panels of the solar cell.

A. Step down Feeding board and STM feeding circuits

A step-down feeding board circuit and an STM feeding circuit are designed. The feeding board circuit used regulator "XC6210B332MR" [19] by taking the output voltage from the other board =5V the regulator output will be 3.3V to feed all sensors and STM as shown in Figure 3. The power distribution switch (STMPS2141STR) is a load switch. For safety reasons, the input power is linked via a pin header and a capacitor. Pin 5 contains the output, which powers the entire circuit. For testing, a Light Emitting Diode (LED) named L1 is connected.

The STM32F405 features a 12-pin "power Connection" to V_{DD}. The step-down feeding STM voltage consisted of 15 capacitors, each with a value of 100 nF were connected in a series connection. Then, 15 pins to one 4.7uF capacitor with a 3.3V output were connected also to give a safe or high voltage enclosure, as shown in Figure 4.

B. Oscillators

The proposed oscillator is designed based on the Pierce oscillator which is frequently employed with a crystal oscillator. The oscillator is designed based on a feedback resistor between the input and output pin and load capacitor [20]. The STM32F405 is compatible with two oscillators The first one of the oscillators worked at 8MHz and has pin 23 as the input pin and pin 24 as the output pin. Each pin of the crystal oscillator (ABM-8.000MHZ-D2Y-T) [21] is connected to a capacitor and resistor common between the two pins. The second oscillator operated at 32MHz, which has pin 8 as the input pin and pin 9 as the output pin, as shown in Figure 5.

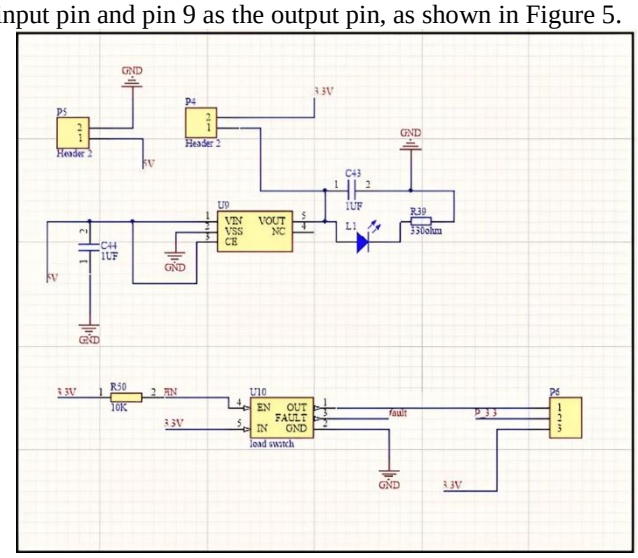

Figure 3. The schematics diagram of the Feeding ADCs board.

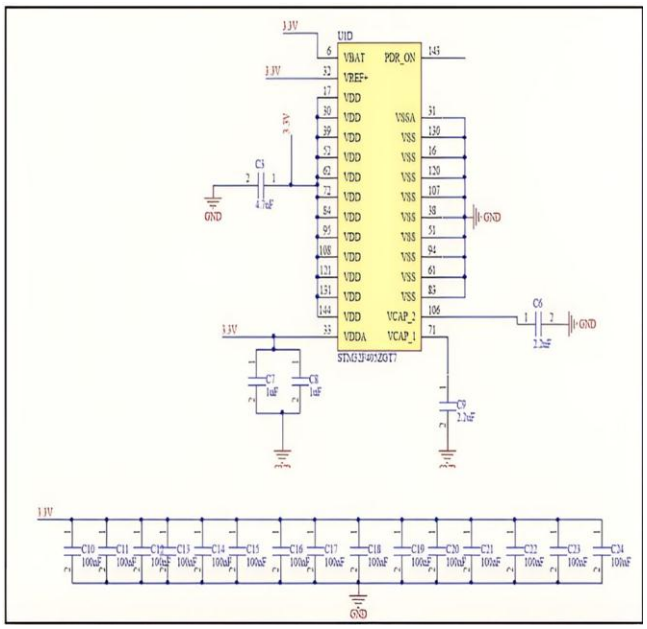

Figure 4. The Schematics diagram of STM32F405 feeding circuit.

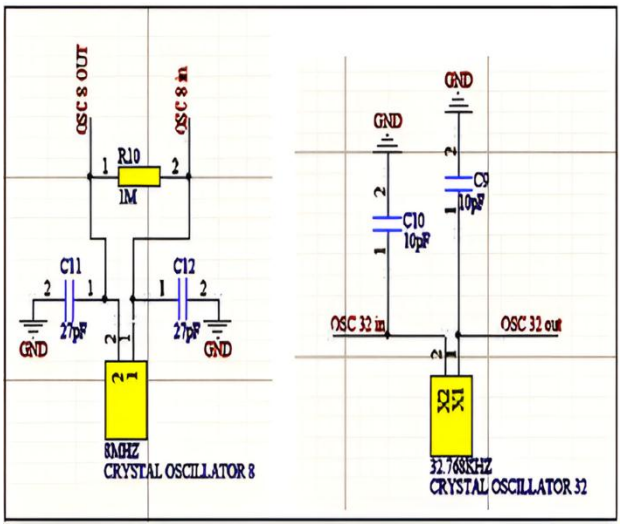

Figure 5. The Schematic diagram of 8MHz and 32 MHz oscillator circuits.

C. Joint Test Action Group

The Joint test action group acted as a connector. J-Tag communicates with processors for programming and debugging devices like microcontrollers, complex programmable logic devices (CPLDs), and field programmable gate arrays (FPGAs). The emulation as a special interface can quickly and easily debug the device. Through software, it can fully control the clock cycles supplied to the microcontroller. As a result, it can be able to implement hardware breakpoints in the code. The hardware's code execution can be started, paused, and stopped whenever you like. The schematic diagram of J-TAG connected to the proposed ADCS board is shown in Figure 6.

DOI: 10.21608/ERJENG.2023.197719.1160

Journal of Engineering Research (ERJ)
Vol. 7 – No. 2, 2023
©Tanta University, Faculty of Engineering
ISSN: 2356-9441 https://erjeng.journals.ekb.eg/ e ISSN: 2735-4873

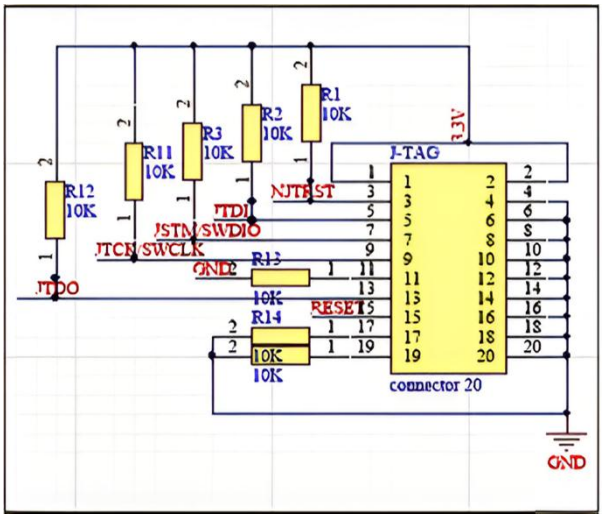

Figure 6. Schematic diagram of the joint test action group using Altuim

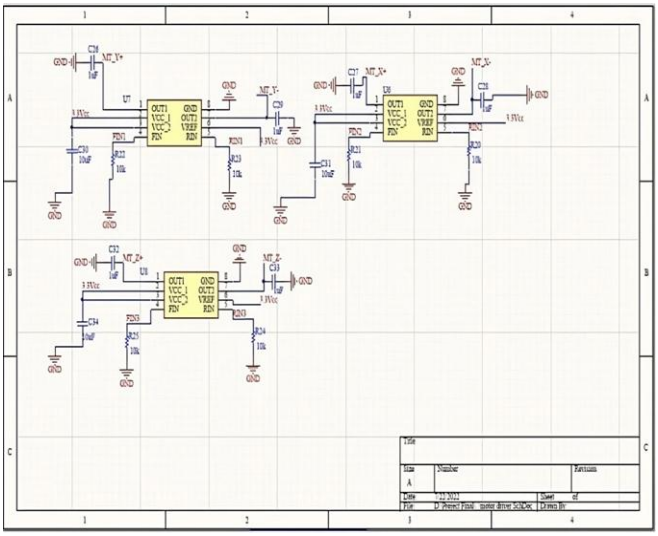

Figure 7. Schematic diagram of the three H-bridge using Altium

D. *Motor diver (H-bridge)*

The three H-bridge drivers (BD6211HFP) [22] are full-bridge drivers intended for use with brush motors. Each IC may function with output currents up to 2A and a power supply operating voltage of 3.0V to 5.5V. PWM speed control is made achievable by MOS transistors in the output stage. The schematic diagram of three H-bridges using the Altium simulator is shown in figure 7.

E. *Pico blade and power amplifier*

The amplifier called the "LM P7704MT" [23] amplifies the voltage produced by the solar cells when they are connected to one another via a pico-blade (53398-1271) [24]. The first one has four inputs and outputs that are fed. Two inputs and two outputs on the second amplifier allow it to generate six outputs from each face utilizing the STM's Analog to Digital Converter (ADC) pins. The schematic diagram of the six pico-blades connected to two amplifiers and as supplied voltage to the ADCS board is shown in Figure 8.

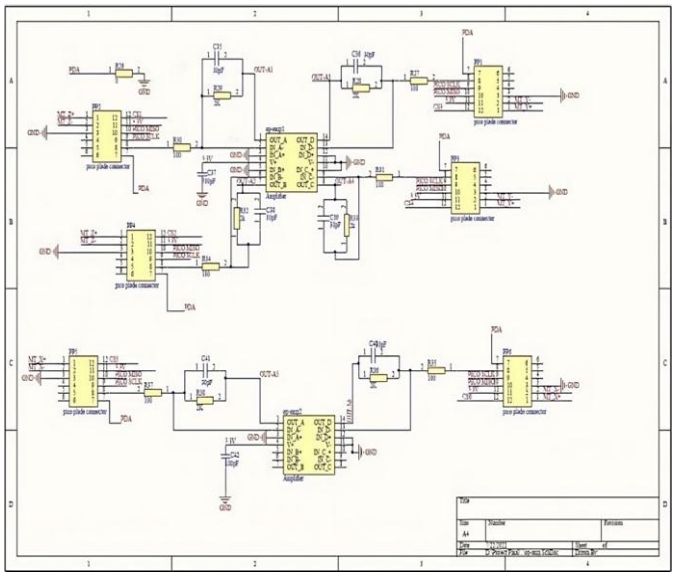

Figure 8. Schematic diagram of the Pico blade and power amplifier using Altium.

III. SENSORS IN ADCS

An array of sensors, actuators, and a backup microcontroller with algorithms make up the ADCS. Following deployment, the goals of ADCS are to reduce the initial random rotation and angular momentum, identify the satellite's current attitude, and either maintain or modify the satellite's attitude based on the information provided by the satellite. The STM32F405 acts as an onboard brain, receiving instructions from various sensors [25-26] to manage attitudes. Temperature sensor "STDS75, [27] used the onboard temperature to determine whether or not it needed to cool. In order to determine the satellite's attitude, the gyroscope "GYRO- A3G4250DTR" [28] measured angular velocity in three coordinates (x, y, and z). The magnetometer RM3100 [29] is used to detect the ambient magnetic field. The simulation of the Gyroscope, temperature and RM3100 magnetometer sensors is shown in Figure 9 using the Altium simulator.

A. *Three-axis digital output gyroscope*

The gyroscope sensor measures angular acceleration, and in order to infer attitude, these observations must be twice integrated [30-31]. The integration causes drifting, which necessitates calibrating. A low-power, three-axis angular rate sensor, the A3G4250D offers remarkable zero-rate stability and temperature and time-dependent sensitivity. The satellite is stabilized by the gyroscope sensor, which also calculates the satellite's rotational speed. Power supply decoupling capacitors (100 nF) ceramic or polyester10μF) should be placed. The A3G4250D IC contains a PLL (phase-locked loop) circuit which synchronizes driving and sensing interfaces. To create a second-order low-pass filter, capacitors, and resistors must be connected to the PLLFILT pin. It consists of a sensing component and an IC interface that may communicate the calculated angular rate to the outside world using a common I2C digital interface. The schematic diagram of the A3G4250D using Altium is shown in Figure 9.

DOI: 10.21608/ERJENG.2023.197719.1160

Journal of Engineering Research (ERJ)
Vol. 7 – No. 2, 2023
©Tanta University, Faculty of Engineering
ISSN: 2356-9441 https://erjeng.journals.ekb.eg/ e ISSN: 2735-4873

B. *Temperature sensor*

The temperature on board was measured to see if it required cooling using the STD875 sensor. The measured temperature value is contrasted with two temperature thresholds: the hysteresis temperature, which is stored in the 16-bit (T_HYS) READ/WRITE register, and a temperature limit, which is kept in the 16-bit (T_os) READ/WRITE register. The device's band gap temperature sensor and programmable 9-to-12-bit ADC allow it to monitor and digitize temperature with a resolution of up to 0.0625 °C. The temperature is translated into a calibrated digital value in degrees Celsius via the inbuilt delta-sigma ADC. The over-limit signal/interrupt alert output (OS/INT) pin becomes active if the measured value goes over certain thresholds. An I2C-compatible serial digital interface and a delta-sigma Analog-to-Digital Converter (ADC) are features of the high-precision CMOS digital temperature sensor. The schematic diagram of the STD875 using Altium is shown in Figure 9.

C. *RM3100 geomagnetic sensor*

The MagI2C ASIC controller and three magneto-inductive sensor coils make up the RM3100 Geomagnetic Sensor. Measurements are intrinsically offset-drift-free and stable throughout the temperature. In order to create an RM3100 Geomagnetic Sensor, each sensor coil acts as the inductive component in a straight forward LR relaxation oscillation circuit, with the coil's effective inductance being proportional to the magnetic field perpendicular to the sensor axis. The measurement concept used an oscillator to detect the ambient magnetic field. The MagI2C ASIC drives the LR circuit, and it measured the oscillation frequency of the circuit and, consequently, the magnetic field using its internal clock. One side of the coil must be grounded in order to conduct a measurement, while the other side must be driven alternately by the positive and negative current through the oscillator. The circuit is operated for a certain number of oscillations, and the internal high-speed clock of the MagI2C is used to calculate how long it takes for each oscillation to finish. The schematic diagram of the RM3100 using Altium is shown in Figure 9.

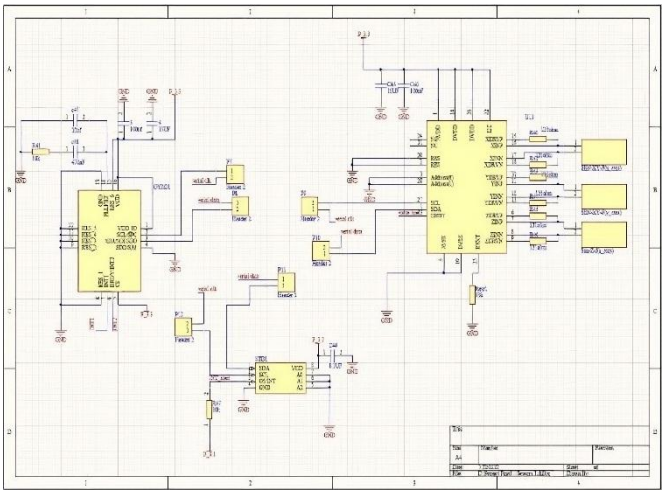

Figure 9. Connection of gyroscope, temperature, and RM3100 geomagnetic sensor using Altium.

IV. IMPLEMENTATION OF THE ADCS BOARD

All circuits of ADCS, as well as the circuitry on the electrical power and sensors, have really been taken into account for the PCB design. The circuits have been placed so that the board takes up the least amount of space possible, and the board's dimensions have been made to match those of the Cube Sat. The PCB layout of the ADCS circuit is implemented based on the Altium software package, as shown in Figure 10. The ADCS-fabricated circuit is presented in Figure 11. The STM32F405 at the center of the board, labeled U1, is connected to the feeding board circuit to step down the supply voltage to 3.3V, and the STM feeding circuit was labeled U9. The two operational amplifiers "LM P7704MT" were called Op1, and Op2, which amplify the voltage produced by the solar cells as the electrical power supply system when they are connected to one another via a 6 Pico-blade labeled PP1 to PP6. The three H-bridge drivers are full-bridge drivers intended for use with brush motors labeled from U6 to U8. The three sensors used in the ADCS board are fabricated and named as Gyroscope, Magnetometer, and Temperature Sensors. They are connected on the board named as GYRO, U11, and STD. The hardware's code execution can be started, paused, and stopped whenever you like using J- TAG connector. Figure 11 shows the fabrication of ADCS based on STM32F405 and external circuit. The proposed circuit board is low-cost, as presented in Table 1.

Table 1: The cost of the ADCS board components.

#	Name	Price
1	STM32F405	250 LE
2	Gyroscope (A3G4250D)	50 LE
3	amplifier (LM P7704MT)	50 LE
4	voltage regulator-Torex XC6210B332MR	25 LE
5	8 MHz oscillator- (ABM-8.000MHZ-D2Y-T)	80 LE
6	D6211HFP (motor driver)	200 LE.
7	Pico blade -53398-1271	20 LE
8	Temperature sensor STDs75	50 LE
9	geomagnetic sensor (RM3100	400 LE

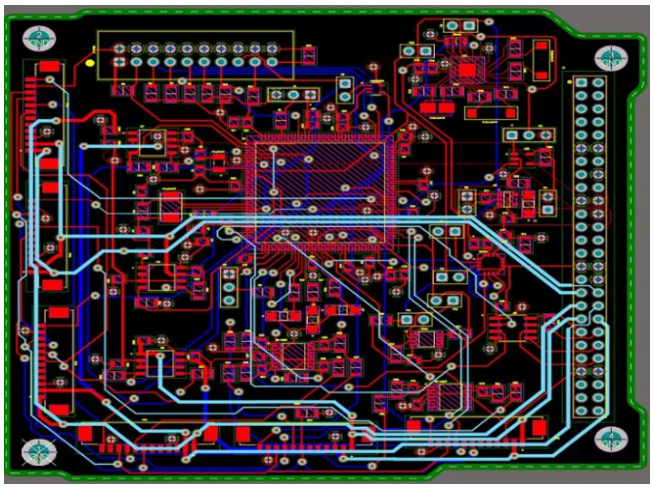

Figure 10. The PCB layout of the ADCS circuit using the Altium software package

DOI: 10.21608/ERJENG.2023.197719.1160

Journal of Engineering Research (ERJ)
Vol. 7 – No. 2, 2023
©Tanta University, Faculty of Engineering
ISSN: 2356-9441 https://erjeng.journals.ekb.eg/ e ISSN: 2735-4873

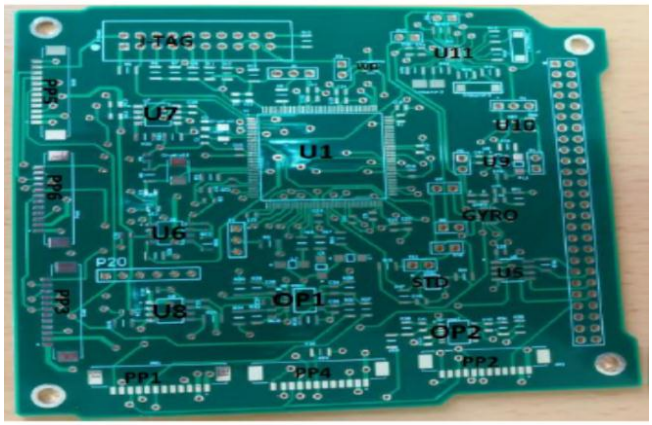

Figure 11. Fabricated ADCS using STM32F405 and connected circuits.

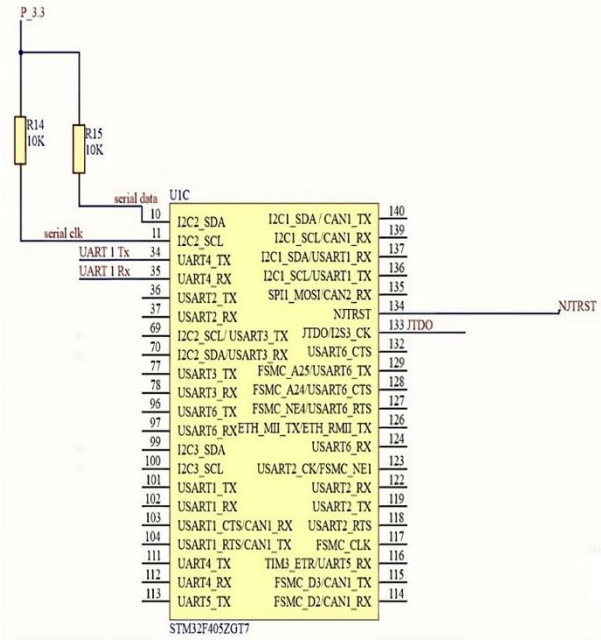

Figure12. The connection pins of communication protocols SPI and I2C are presented at the STM32F405.

V. SOFTWARE INTERFACE OF ADCS

The software program of this study is based on interfacing between hardware and ARM microcontroller and is devoted to creating the code and method for reading the sensors connected with the STM32 microcontroller. The reading of Gyroscope sensor is main reading sensor to detect the attitude determination in three axes. STM32F405 microcontroller in our board is programmed based on the J-TAJ interface connection pin by debugging through SPI (synchronous Serial Peripheral Interface) communication protocol. Separate wires for the clock line and data line are needed in SPI. The clock must be supplied as a separate signal because it is not part of the data stream. In SPI registers, the data transmission is set up. Sensor and STM connections are made using I2C pins. The data from STDS75 and A3G4250D sensors are read using the I2C communication protocol.

The two I2C pins are used to link all of the sensors to the microcontroller at pins number 10 for serial data and pin number 11 for the serial clock, as illustrated pins in Figure 12, the communication protocol I2C is divided into I2C clock and I2C data. As shown in Figure 13, the output of the temperature sensor reading 26 is presented as (0X1A). The gyroscope is a sensor that is used to determine the satellite's speed, which is communicated based on the I2C protocol. The A3G4250D always communicates with the STM32 controller system as a slave device to check the attitude measurement. The satellite is stabilized by the gyroscope sensor, which also calculates the satellite's rotational speed. The main in the proposed is to measure the attitude determination. The figure 14 is represented the real-time measurement of the attitude determination of the satellite based on a gyroscope sensor in 3-axis direction. The attitude data measurement is used to calibrate the attitude of the satellite based on a microcontroller.

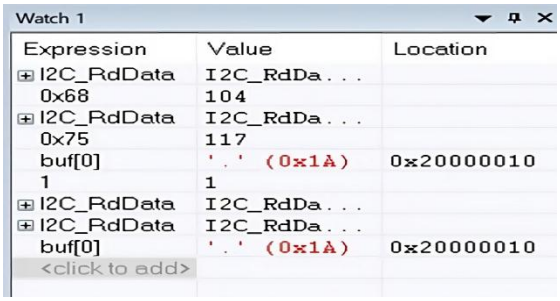

Figure 13. The output of the temperature sensor at 〖26〗^0 C.

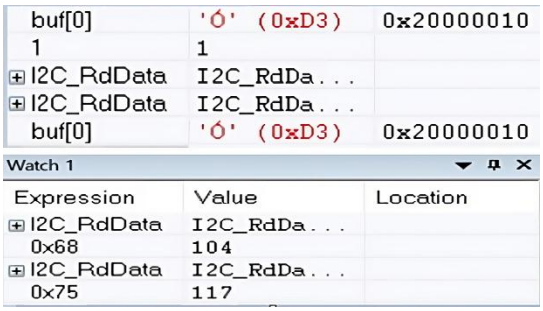

Figure 14. The output of the gyroscope sensor speed in three directions is based on the communication protocol.

VI. CONCLUSION

A small-dimension hardware implementation of ADCS is presented in this work. The suitable microcontroller and sensors subsystems are implemented in the ADCS board. The STM32F405 from the ARM family is used as a suitable microcontroller subsystem for the ADCS board. The sensors subsystem implemented the gyroscope, magnetometer, and temperature sensors to measure angular velocity, ambient magnetic field, and temperature of the proposed board. The external circuits are designed and implemented to be suitable for the microcontroller and feeding ADCS board. The supply voltage circuit is implemented based on six pico-blade connectors connected with two amplifiers to amplify the output voltage from six solar cell panels. The step-down circuits are divided into step-down feeding ADCS board and step-down STM32 feeding to create a suitable feeding supply voltage. The two oscillators that are needed in the STM32F05 are designed. The three H-bridge drivers are full-bridge drivers intended for use with brush motors. A joint action group (J-Tag) used as easily debug the device. Our ADCS board is

DOI: 10.21608/ERJENG.2023.197719.1160

Journal of Engineering Research (ERJ)
Vol. 7 – No. 2, 2023
©Tanta University, Faculty of Engineering
ISSN: 2356-9441 https://erjeng.journals.ekb.eg/ e ISSN: 2735-4873

simulated using Altium and fabricated in a printed circuit board (PCB). The software program of this proposal is based on interfacing between hardware and ARM microcontroller. The small dimensions of ADCS are achieved in dimensions 10×9.7 cm^2 that are compatible with Cubesat. Our ADCS board is successfully simulated and tested for reading gyroscope and temperature sensors.

Acknowledgment

This paper is part of the CubeSat project at the Egyptian Space Agency. We want to thank the following technical engineers for their work on the project: Ibrahim Ahmed Mohamed Ahmed, Karim Hesham Abd-ElFattah Abd-ElHady.

Funding: No funds were used to perform the research.

Conflicts of Interest: There is no conflict of interest, according to the Authors understanding.

REFERENCES

[1] Sweeting, M. N. (2018), 'Modern small satellites-changing the economics of space', Proceedings of the IEEE 106(3), 343–361
[2] T. C. Program. "CubeSat design specification rev 14.1." Feb. 2022. [Online]. Available: http://cubesat.org/ (last access date 15/3/2023)
[3] L. R. Abramowitz, "US Air Force's SMC/XR SENSE NanoSat program," in AIAA SPACE 2011 Conference & Exposition, Long Beach, CA, USA, September 2011.
[4] J. London, M. Ray, D. Weeks, and B. Marley, "The first US army satellite in fifty years: SMDC-ONE first flight results," in 25th Annual AIAA/USU Conference on Small Satellites, London, 2011.
[5] S. Padmanabhan, S. Brown, P. Kangaslahti, et al., "A 6U Cube-Sat constellation for atmospheric temperature and humidity sounding," in 27th Annual AIAA/USU Conference on Small Satellites, Padmanabhan, 2013.
[6] Michael Swartwout, Miguel Nunes, and Vaios Lappas "CubeSats and Small Satellites" Vol.2019, https://doi.org/10.1155/2019/9451673
[7] K. Nakaya, K. Konoue, H. Sawada, et al., "Tokyo Tech CubeSat: CUTE-I - Design & Development of Flight Model and Future Plan," in 21st International Communications Satellite Systems Conference and Exhibit, Yokohama, Japan, April 2003.
[8] J Straub and D. Whalen, "Evaluation of the educational impact of participation time in a small spacecraft development program," Education in Science, vol. 4, no. 1, pp. 141–154, 2014.
[9] Neeck SP., "Small Satellites and NASA Earth Science", presented at the 11th IAA Symposium on Small Satellites for Earth Observation, Berlin, Germany, 2017.
[10] Fritz M, Shoer J, Singh L, Henderson T, McGee J, Rose R, Ruf C., "Attitude determination and control system design for the CYGNSS microsatellite", in 2015 IEEE Aerospace Conference, Mar. 2015, pp. 1–12.
[11] Fritz M, Shoer J, Singh L, Henderson T, McGee J, Rose R, Ruf C (2019) Attitude determination and control system design for the CYGNSS microsatellite. In: 2019 IEEE aerospace conference. Pp 1–12. https://doi.org/10.1109/AERO.2019.8742161.
[12] Tassano M, Monzon P, Pechiar J. "Attitude determination and control system of the Uruguayan CubeSat, AntelSat," 2013 16th International Conference on Advanced Robotics (ICAR), Montevideo, 2013, pp. 1-6.
[13] F. Landis Markley, John L. Crassidis "Fundamentals of spacecraft Attitude Determination and control", Published jointly by Microcosm Press and Springer, 2019
[14] KAPLAN, CEREN, Leo Satellites: Attitude Determination and Control Components; Some Linear Attitude Control Techniques, Dissertation, Middle East Technical University, 2006.
[15] Daniel D. Kekez, Robert E. Zee, and Freddy M. Pranajaya. Launches and On-Oribt Performance: An Update on Nanosatellite Missions at the UTIAS Space Flight Laboratory. Space Flight Laboratory, University of Toronto, 2010.
[16] Khaled Gaber · Mohamed B. El Mashad · Ghada A. Abdel Aziz " Hardware-in-the-loop real-time validation of micro-satellite attitude control" Computers and electrical engineering, Vol. 85, July, 2020.
[17] Khaled Gaber · Mohamed B. El Mashad · Ghada A. Abdel Aziz, "A Hardware Implementation of Flexible Attitude Determination and Control System for Two Axis Stabilized CubeSat" Journal of Electrical Engineering & Technology (2020) 15:869–882.
[18] STM32F405 URL: (https://www.st.com/en/microcontrollers-microprocessors/stm32f405-415.html) (last access 15/12/2022)
[19] Voltage regulator, Torex XC6210B332MR URL: (https:// octopart. com/xc6210b332mr-torex-5397250) (last access 15/11/2022)
[20] E. Vittoz High-Performance Crystal Oscillator Circuits: Theory and Application IEEE Journal of Solid-State Circuits, Vol 23, No 3, June 1988 pp 774 - 783.
[21] Crystal oscillator (ABM-8.000MHZ-D2Y-T) URL: https://eu.mouser.com/ProductDetail/ABRACON/ABM7-8.000MHZ-D2Y-T?qs=LoTOQoUkC8SFsmY8snleBA%3D%3D) (last access 15/11/2022)
[22] Motor driver (D6211HFP) URL: (https://www.rohm.com/products/motor-actuator-rivers/dc-brush-motor/bd6211hfp-product#productDetail). (last access date 15/10/2022).
[23] Operational-amplifier(LMP7704MT) URL: (https://www.ti.com/product/LMP7704/part-details/LMP7704MT/NOPB). (last access date 20/10/2022).
[24] Pico blade (53398-1271) URL: (https://www.molex.com/molex/products/part-detail/pcb_headers/0533981271#). (Last access date 10/12/2022)
[25] Horri, N.M., Palmer, P., Giffen, A.: Active attitude controlmechanisms. In: Blockley, R., Shyy, W. (eds.) Encyclopedia of Aerospace Engineering. Wiley, Chichester (2010).
[26] Merhav, S.: Aerospace Sensor Systems and Applications. Springer, New York (1962)
[27] Temperature sensor STDs75 URL: (file:///C:/Users/user/Downloads/stds75.pdf). (Last access date 10/11/2022).
[28] 3- axis Gyro (A3G4250DTR) URL: (https://eu.mouser.com/datasheet/2/389/a3g4250d-1849040.pdf). (Last access date 10/11/2022)
[29] Geomagnetic sensor (RM3100) (Last access date 10/10/2022) URL:(https://www.terraelectronica.ru/pdf/show?
[30] Fallon III, L.: Gyroscopes. In: J.R. Wertz (ed.) Spacecraft Attitude Determination and Control, chap. 6.5. Kluwer Academic, Dordrecht (1978)
[31] Pittelkau, M.E.: Sensors for attitude determination. In: Blockley, R., Shyy, W. eds.) Encyclopedia of Aerospace Engineering. Wiley, Chichester (2010).

DOI: 10.21608/ERJENG.2023.197719.1160